具有任意形狀切塊區域之層疊板的挫屈與振動問題之數值解

洪志強、廖惠雯、黃明鋒、簡國璋

摘要

非等向性長方形層疊板具有對稱於厚度中間面的任意形狀之切塊區域，分別在四邊簡支和固支邊界條件下，將切塊區域所剩下的部分視爲一具有減少勁度之均勻板，來做單純整體挫屈與振動的研究。板勁度的變化以溥立葉級數來表示。我們以理茲(Ritz)的能量原理方法來求層疊板被切任意形狀之切塊後在受軸向壓縮力作用下的電腦數值計算解。在圓形和橢圓形切塊區域的減少勁度之數值解已經得到。我們發現單純整體挫屈負載隨著切塊區域增加而減少，基本頻率也隨著切塊區域增加而減少。

關鍵詞：單純整體挫屈，切塊區域，減少勁度，任意形狀。

洪志強：修平技術學院資訊管理系助理教授
廖惠雯：嶺東技術學院資訊管理系助理教授
黃明鋒：大葉大學共同教學中心副教授
簡國璋：中興大學應用數學系教授

Numerical Solution of Buckling and Vibration in Laminates with Arbitrary Shape Cut Off Regions

C. C. Hong，H. W. Liao，M. F. Hwang，K. C. Jane

Abstract

The pure global buckling and vibration of four sides simply-supported as well as clamped anisotropic laminates having an arbitrary shape cut off region that is symmetric with respect to mid-plane have been studied by treating the remaining cut off regions as uniform plates with reduced stiffness. The variation of stiffness of the plate is represented by Fourier series. Computational solutions of the energy principle for the Ritz method in a plate having arbitrary shape of typical cut off regions under biaxial compressive loads are obtained. Some numerical results for the pure global buckling load prediction due to its reduced flexural stiffness for the circular cut off regions and elliptical cut off regions are presented. We find the normalized pure global buckling load ratio decreases as the cut off regions size increases, and the nondimensional fundamental frequency value decreases as the cut off regions size increases.

Key words: pure global buckling, cut off region, reduced stiffness, arbitrary shape.

C. C. Hong : Assistant Professor, Department of Information Management, HIT
H. W. Liao : Assistant Professor, Department of Information System, Ling Tung College
M. F. Hwang : Associate Professor, Liberal Art Center, Da Yeh University
K. C. Jane : Professor, Department of Applied Mathematics, National Chung Hsing University

1. Introduction

Many researchers have studied various aspects of buckling load and free vibration of plates with and without the delaminations analytically and experimentally [1-5]. There are three possible buckling mode types: (a) local buckling mode, (b) global buckling mode and (c) coupled global and local buckling modes that have been examined. Cut off regions on the top and bottom surfaces of laminated plate may be necessary for fitting something on it. Cut off regions may reduce bending stiffness of laminates, which lower the compressive load carrying capacity and natural frequencies. In 2000, Jane and Hong [6] made a study about the pure global buckling and vibration of rectangular laminates with rectangular cut off regions. An energy approach for the Ritz procedure was discussed by Whitney [7] is used to determine the pure global buckling load and vibration of four edges simply-supported as well as clamped anisotropic rectangular laminates that having arbitrary shape cut off regions.

The stiffness variation of the plate is represented by Fourier series [5] and the partition technique [8] can be utilized to approach the arbitrary shape of cut off regions into the rectangular subregions and right triangular subregions. The Ritz method using the reduced flexural stiffnesses to represent the stiffness of the arbitrary shape of cut off regions under biaxial compression loads would be studied. The purpose of this study is to investigate the effect of arbitrary shape cut off regions to the pure global buckling and vibration of rectangular plates by energy method. The typical anisotropic rectangular laminates with middle-plane symmetric arbitrary shape cut off region that is shown in Figure 1. With coordinates $X_1(x_1,y_1)$, $X_2(x_3,y_1)$, $X_3(x_3,y_4)$, $X_4(x_2,y_3)$ and $X_5(x_1,y_2)$ and is used to demonstrate the study procedures. We partition the arbitrary shape of cut off region into the rectangular subregions and right triangular subregions as shown in Figure 2. Where $\zeta_{(k)}$ is the x-coordinate at middle point of $2c_{(k)}$,$2c_{(k)}$, which is the x-directional length of cut off

sub-region and $\eta_{(l)}$ is the y- coordinate at middle point of $2d_{(l)}$,$2d_{(l)}$, which is the y-directional length of cut off sub-region.

2. Formulation

2.1 Governing equation

The strain energy of an elastic plate in terms of Cartesian coordinates x, y system is written in the following relationship [7]:

$$U = \frac{1}{2}\iint(\sigma_x\varepsilon_x + \sigma_y\varepsilon_y + \sigma_{xy}\varepsilon_{xy})dxdy \qquad (1)$$

where σ_x and σ_y are the normal stresses, σ_{xy} is the shear stress, ε_x and ε_y are the normal strains, and ε_{xy} is the shear strain. This strain energy generally contains two parts of energy, there are strain energy due to stretching and strain energy due to bending. By substituting the plane stress constitutive equations and the strain-displacements relations into relationship equation (1), we find that the strain energy for pure transverse bending of anisotropic laminated plate can be written in the following equation:

$$U = \frac{1}{2}\iint[\bar{D}_{11}(\frac{\partial^2 W}{\partial x^2})^2 + 2\bar{D}_{12}\frac{\partial^2 W}{\partial x^2}\frac{\partial^2 W}{\partial y^2} + \bar{D}_{22}(\frac{\partial^2 W}{\partial y^2})^2 + 4\bar{D}_{66}(\frac{\partial^2 W}{\partial x\partial y})^2 + 4(\bar{D}_{16}\frac{\partial^2 W}{\partial x^2} + \bar{D}_{26}\frac{\partial^2 W}{\partial y^2})\frac{\partial^2 W}{\partial x\partial y}]dxdy \qquad (2)$$

where W is the transverse displacement, $\bar{D}_{ij}$ are the flexural stiffnesses.

The potential energy of external inplane loads due to a transverse deflection is given as follows:

$$V = \iint(N_x^i\varepsilon_x^0 + N_y^i\varepsilon_y^0 + N_{xy}^i\varepsilon_{xy}^0)dxdy \qquad (3)$$

where N_x^i, N_y^i and N_{xy}^i are initial external inplane force resultants applied to the rectangular plane in a prebuckled state, ε_x^0, ε_y^0 and ε_{xy}^0 are the midplane strains due to the transverse deflection. We consider the initial axial loads acting on the plane in the x- and y- directions, these external loads are represented as:

$$N_x^i = P_x, N_y^i = P_y, N_{xy}^i = 0 \qquad (4)$$

For considering the large transverse deflection in the buckled state, we have nonlinear terms in the strains involving

transverse displacement W as follows:

$$\varepsilon_x^0 = \frac{1}{2}\left(\frac{\partial W}{\partial x}\right)^2, \varepsilon_y^0 = \frac{1}{2}\left(\frac{\partial W}{\partial y}\right)^2, \varepsilon_{xy}^0 = \frac{\partial W}{\partial x}\frac{\partial W}{\partial y} \quad (5)$$

By substituting equations (4) and (5) into equation (3), we arrive at the following potential energy equation:

$$V = \frac{1}{2}\iint\left[P_x\left(\frac{\partial W}{\partial x}\right)^2 + P_y\left(\frac{\partial W}{\partial y}\right)^2\right]dxdy \quad (6)$$

The kinetic energy of an elastic plane in terms of a Cartesian coordinate x, y, z system is written in the following relationship:

$$T = \frac{1}{2}\iiint\rho_0^{(k)}\left[\left(\frac{\partial u}{\partial t}\right)^2 + \left(\frac{\partial v}{\partial t}\right)^2 + \left(\frac{\partial W}{\partial t}\right)^2\right]dxdydz \quad (7)$$

where $\rho_0^{(k)}$ is the density of the k-th layer in laminated plate, u,v and W are the displacement components in the x, y and z directions respectively, t is the time. For considering the tangential displacement u,v are linear functions of the z coordinate and neglecting the rotatory inertia terms, after integrating with respect to z, we have the following expression:

$$T = \frac{1}{2}\iint\rho h\left[\left(\frac{\partial u^*}{\partial t}\right)^2 + \left(\frac{\partial v^*}{\partial t}\right)^2 + \left(\frac{\partial W^*}{\partial t}\right)^2\right]dxdy \quad (8)$$

where ρ is density of the laminated plate, h is thickness of the rectangular plate, and u^0,v^0 are the displacement components of the mid-plane. Conventionally, we consider the vibration under the following displacement forms:

$$u^* = u^0 e^{i\omega t}, v^* = v^0 e^{i\omega t}, W^* = W(x,y)e^{i\omega t} \quad (9)$$

where ω is a natural frequency of vibration. By putting equation (9) into equation (8), the kinetic energy can be rewritten as:

$$T = \frac{1}{2}\iint\rho h\omega^2\left(u^{0^2} + v^{0^2} + W^2\right)dxdy \quad (10)$$

2.2 Energy principle

The energy principle for the Ritz procedure can be stated as [7]:

$$\Pi(u^0, v^0, W) = U + V - T = \text{stationary value} \quad (11)$$

where Π is Lagrangian functional, U is the bending strain energy, V is the potential

energy of inplane loads, and T is the kinetic energy of the laminated plate. By considering bending and linear inertia of the plate, equation (11) becomes:

$$\Pi = \frac{1}{2}\int_0^a\int_0^b [\bar{D}_{11}(\frac{\partial^2 W}{\partial x^2})^2 + 2\bar{D}_{12}\frac{\partial^2 W}{\partial x^2}\frac{\partial^2 W}{\partial y^2} + \bar{D}_{22}(\frac{\partial^2 W}{\partial y^2})^2 + 4\bar{D}_{66}(\frac{\partial^2 W}{\partial x \partial y})^2 + 4\bar{D}_{16}\frac{\partial^3 W}{\partial x^3}\frac{\partial^3 W}{\partial x \partial y} + 4\bar{D}_{26}\frac{\partial^3 W}{\partial y^3}\frac{\partial^3 W}{\partial x \partial y} + P_x(\frac{\partial W}{\partial x})^2 + P_y(\frac{\partial W}{\partial y})^2 - \rho h\omega^2(u^2 + v^2 + W^2)]dxdy \quad (12)$$

where a and b are dimensions of the rectangular plate, $\bar{D}_{11}, \bar{D}_{12}, \bar{D}_{66}$ and $\bar{D}_{22}$ are the flexural stiffnesses and $\bar{D}_{16}, \bar{D}_{26}$ are the bending-twisting coupling stiffnesses of the laminate, P_x and P_y are applied biaxial loads in x- and y- directions respectively.

2.3 Reduced flexural stiffness

When the arbitrary shape of cut off region is occurred in the rectangular plate, the overall effective flexural stiffness would be smaller than the flexural stiffness of perfect plate. We would like to partition the arbitrary shape of cut off region into sufficient numbers of rectangular shape of subregions and right triangular shape of subregions to get the approximate solution. A double Fourier series form of reduced flexural stiffnesses $\{\bar{D}\} = \{D\}f(x,y)$ had been used in the delaminated plate study by Wang et al [5]. With $\{D\}$ representing original stiffnesses $D_{11}, D_{12}, D_{66}, D_{16}, D_{26}$ and D_{22} and the distribution function of reduced flexural stiffnesses is written in the following form:

$$f(x,y) = a_{00} + \sum_{i=1}^{\infty} a_{i0}\cos\alpha_i x + \sum_{j=1}^{\infty} a_{0j}\cos\beta_j y + \sum_{i=1}^{\infty}\sum_{j=1}^{\infty} a_{ij}\cos\alpha_i x\cos\beta_j y \quad (13)$$

where a_{00}, a_{i0}, a_{0j} and a_{ij} are the Fourier coefficients, they are written in the following forms for the arbitrary shape of approximately cut off region that is shown in Figure 2:

$$a_{00} = 1 - \frac{1}{A}\sum_{u}^{u1} A_u(1 - R_u) - \frac{1}{A}\sum_{w}^{tR1} TA_w(1 - R_w)$$

$$a_{i0} = \frac{2}{a}\sum_{i=0}^{i} \int_{\eta_{i-1}+\varepsilon_{i-1}}^{\eta_i+\varepsilon_i} \cos\alpha_i x dx + \frac{2}{a}\sum_{i=1}^{i'} \int_{\eta_{i-1}+\varepsilon_{i-1}}^{\eta_i+\varepsilon_i} [1 - \frac{2}{b}\sum_{j=1}^{j_i} d_{(i)j}(1 - R_{uj})]\cos\alpha_i x dx + \frac{2}{a}\sum_{i}^{i''} \int_{\eta_{i-1}-\varepsilon_{i-1}}^{\eta_i-\varepsilon_i} [-\frac{1}{b}\sum_{j=1}^{j_i''} \frac{d_{(i)j}}{c_{(i)j}}(x - \xi_{(i)j} + c_{(i)j})(1 - R_{uj})]\cos\alpha_i x dx$$

$$a_{0j} = \frac{2}{b}\sum_{j=0}^{j} \int_{\xi_j+d_j}^{\xi_{j+1}-d_{j+1}} \cos\beta_j y dy + \frac{2}{b}\sum_{j=1}^{j'} \int_{\xi_{j-1}+d_{(j)1}}^{\xi_j-d_{(j)1}} [1 - \frac{2}{a}\sum_{k=1}^{k_j} c_{(j)k}(1 - R_{uk})]\cos\beta_j y dy + \frac{2}{b}\sum_{j}^{j''} \int_{\xi_{j-1}-d_{(j)1}}^{\xi_j+d_{(j)1}} [\frac{1}{a}\sum_{k=1}^{k_j''} \frac{c_{(j)k}}{d_{(j)k}}(y - \eta_{(j)k} - d_{(j)k})(1 - R_{uk})]\cos\beta_j y dy$$

$$a_{ij} = \frac{4}{ab}\int\sum_{k=1}^{K}\int_{\cdots}^{\cdots}\cos\alpha_i x\cos\beta_j y dxdy + \frac{4}{ab}\sum_{k=1}^{K}\Big(\int_{\cdots}^{\cdots}\sum_{l=1}^{L}\int_{\cdots}^{\cdots}\cos\alpha_i x\cos\beta_j y dxdy + \int_{\cdots}^{\cdots}\sum_{l=1}^{L}\int_{\cdots}^{\cdots}R_{kl}\cos\alpha_i x\cos\beta_j y dxdy\Big) + \frac{4}{ab}\sum_{k=1}^{TK}\Big\{\int_{\cdots}^{\cdots}\sum_{l=1}^{TK_k}\int_{\cdots}^{\cdots}\Big[1+\frac{c_{(k)}}{d_{(l)}}(y-\eta_{(l)}-d_{(l)})\Big](1-R_{kl})\Big\}\cos\alpha_i x\cos\beta_j y dxdy\Big\} \quad (14)$$

where $\alpha_i = i\pi/a$, $\beta_j = j\pi/b$, A_{kl} is the area of the kl^{th} cut off rectangular sub-region of $2c_{(k)}$ by $2d_{(l)}$ dimensions with its center at $(\xi_{(k)}, \eta_{(l)})$ as shown in Figure 2, KL is the total number of cut off rectangular subregions, $A=ab$, R_{kl} is the ratio of the amount of flexural stiffnesses, same for all components, for the kl cut off sub-region to the corresponding stiffnesses of the no cut of laminate,$\zeta_0 = c_0 = 0$,$\zeta_2 = a$, $c_2 = 0$, $\eta_2 = b$,$d_2 = 0$, K is the total number of cut off rectangular sub-regions in the x-direction. At each $\xi_{(k)}$, there are L_k cut off rectangular subregions, L is the total number of cut off rectangular sub-regions in the y-direction. At each $\eta_{(l)}$, there are K_l cut off rectangular subregions. TA_{kl} is the area of the kl^{th} cut off right triangular subregion of $2c_{(k)}$ by $d_{(l)}$ dimensions with $(\xi_{(k)}, \eta_{(l)})$ at the middle point of sidelong edge, TKL is the total number of cut off right triangular subregions, TK is the total number of cut off right triangular sub-regions in the x-direction. At each $\xi_{(k)}$, there are TL_k cut off right triangular subregions, TL is the total number of cut off right triangular subregions in the y-direction. At each $\eta_{(l)}$, there are TK_l cut off right triangular subregions. For the closely representing $f(x, y)$ to actual stiffness, a sufficient number of terms of a_{ij} would be used. Of course, only $a_{00} = 1$ exists if there is no cut off region.

2.4 The Ritz method

The Ritz method provides a convenient method for obtaining approximate solutions for buckling and/or vibration problems. For the present problem of four sides simply supported, and four sides clamped rectangular anisotropic plates with arbitrary shape of cut off region, the solution is assumed in the following form:

$$W = \sum_{m=1}^{M}\sum_{n=1}^{N} W_{mn} X_m(x) Y_n(y) \quad (15)$$

and for the reduced flexural stiffnesses $\{\overline{D}\}=\{D\}f(x,y)$ in cut off plate, with the process of minimization equation [7]:

$$\frac{\partial \Pi}{\partial W_{mn}}=0, \quad \begin{matrix}m=1,2,\ldots,M\\ n=1,2,\ldots,N\end{matrix} \tag{16}$$

Substituting equation (15) in conjunction with equation (13) into equation (16), we arrive at:

$$\begin{aligned}
&\sum_{i=1}^{M}\sum_{j=1}^{N}\{\int\int D_{11}f(x,y)\frac{d^2X_i}{dx^2}\frac{d^2X_m}{dx^2}Y_jY_n\,dxdy+\\
&\int\int D_{12}f(x,y)\{X_m\frac{d^2X_i}{dx^2}Y_j\frac{d^2Y_n}{dy^2}+X_i\frac{d^2X_m}{dx^2}Y_n\frac{d^2Y_j}{dy^2}\}dxdy+\\
&\int\int D_{22}f(x,y)\{X_iX_m\frac{d^2Y_j}{dy^2}\frac{d^2Y_n}{dy^2}\}dxdy+\\
&\int\int 4D_{66}f(x,y)\{\frac{dX_i}{dx}\frac{dX_m}{dx}\frac{dY_j}{dy}\frac{dY_n}{dy}\}dxdy+\\
&\int\int 2D_{16}f(x,y)\{\frac{d^2X_i}{dx^2}\frac{dX_m}{dx}Y_j\frac{dY_n}{dy}+\frac{dX_i}{dx}\frac{d^2X_m}{dx^2}Y_n\frac{dY_j}{dy}\}dxdy+\\
&\int\int 2D_{26}f(x,y)\{X_m\frac{dX_i}{dx}\frac{dY_j}{dy}\frac{d^2Y_n}{dy^2}+X_i\frac{dX_m}{dx}\frac{d^2Y_j}{dy^2}\frac{dY_n}{dy}\}dxdy+\\
&P_x\int\frac{dX_i}{dx}\frac{dX_m}{dx}dx\int Y_jY_n\,dy+\\
&P_y\int X_iX_m\,dx\int\frac{dY_j}{dx}\frac{dY_n}{dx}dy-\\
&\rho h\omega_{mn}^2\int X_iX_m\,dx\int Y_jY_n\,dy\}W_{mn}=0, \quad \begin{matrix}i=1,2,\ldots,M\\ j=1,2,\ldots,N\end{matrix}
\end{aligned} \tag{17}$$

in which $f(x,y)$ represents the distribution function of bending stiffness and bending-twisting coupling stiffness of the plate. Although $f(x,y)$ could be different for different stiffness components, it is taken to be uniform for all in the present study. After integrating equation (17) with properly assumed $X_m(x)$ and $Y_n(y)$, we have the following system of equations.

$$[A]_{M\times N}\{W\}=0 \tag{18}$$

in which $[A]_{M\times N}$ contains P_x and/or ω_{mn} with specified P_y/P_x as parameters. By requiring the determinant of the coefficient matrix in equation (18) to vanish, we have the eigenvalue problem for the critical P_x or ω_{mn}, or ω_{mn} under a given P_x.

2.5 Simply-supported rectangular plate

We now consider the simply supported rectangular laminated plate compressed by uniform inplane loads of P_x with specified P_y/P_x. The boundary conditions for a four edges simply-supported rectangular plate are written as follows:

$$W=\partial^2W/\partial x^2=0 \quad \text{at} \quad x=0,a \tag{19}$$
$$W=\partial^2W/\partial y^2=0 \quad \text{at} \quad y=0,b \tag{20}$$

and the following characteristic functions

for $X_m(x)$ and $Y_n(y)$ are selected.

$$X_m(x) = \sin \alpha_m x = \sin \frac{m\pi x}{a}$$
$$Y_n(y) = \sin \beta_n y = \sin \frac{n\pi y}{b} \qquad (21)$$

By substituting the equation (13) and (21) into equation (17), and performing integrations afterwards, we can obtain the equations in series forms.

2.6 Clamped rectangular plate

We consider a four sides clamped rectangular laminated plate compressed by uniform inplane loads of P_x with specified P_y/P_x. The boundary conditions are:

$$W = \partial W/\partial x = 0 \quad \text{at} \quad x = 0, a \qquad (22)$$
$$W = \partial W/\partial y = 0 \quad \text{at} \quad y = 0, b \qquad (23)$$

and the following characteristic functions for $X_m(x)$ and $Y_n(y)$ are selected.

$$X_m(x) = 1 - \cos 2\alpha_m x = 1 - \cos \frac{2m\pi x}{a}$$
$$Y_n(y) = 1 - \cos 2\beta_n y = 1 - \cos \frac{2n\pi y}{b} \qquad (24)$$

By substituting the equation (13) and (24) into equation (17), and performing integrations afterwards, we also can obtain the equations in series form.

3. Some numerical results and discussions

We assumed that there were no local buckling occurred in the anisotropic laminates under the whole processes of axial compression in the numerical simulations. The stiffness of a remaining middle-plane symmetrical cut off region is determined by the flexural stiffness between every two adjacent cut off region, through the thickness of the plate. For example, if there is a middle-plane symmetrical single cut off region through the thickness as shown in Figure 3, we have $R_{kl} = (1 - \frac{h_1}{h} - \frac{h_2}{h})^3$. Firstly, we study the convergence of pure global buckling solution for a simply supported plate with arbitrary shape of typical cut off region as shown in Figure 1 with the coordinates $X_1(0.2b,0.2b)$, $X_2(0.8b,0.2b)$, $X_3(0.8b,0.8b)$, $X_4(0.5b,0.6b)$, $X_5(0.2b,0.4b)$, i.e., $c_1 = d_1 = 0.3b$, $\xi_1 = \eta_1 = 0.5b$ and $h_1/h = 0.3$ is shown in Figure 4a. And convergence of pure global buckling solution for a clamped

plate with the same coordinates of arbitrary shape of typical cut off region is shown in Figure 4b. We find the total number of terms resulting in a *M=N=5* of [*A*] matrix is established explicitly and used to demonstrate the calculating procedure. The typical stiffness for the perfect part is taken to be $D_{22}=1$, $D_{11}=D_{33}$, $D_{12}+2D_{66}=2.38D_{22}$, $D_{16}=D_{26}=0.69D_{22}$ for all numerical computations. Secondly, we study the following cut off region cases:

3.1 Typical cut off region case

3.1.1 Simply supported plate

A plate with arbitrary shape of typical cut off region (see Figure 1) with the coordinates under biaxial loading condition with $P_x=P_y=P$ is considered. The following buckling load parameter is introduced: $P^*_{cr}=(P_x b^2)/(D_{22}\pi^2)$. The result for the critical load of a plate without cut off region by using the Ritz method is found to be 3.0396, which should be the maximum upper bound for all other numerical results presented in this paper.

A square plate has arbitrary shape of typical cut off region with y-coordinates $y_1=0.2b$, $y_2=0.4b$, $y_3=0.6b$, $y_4=0.8b$ (fixed $d_1=0.3b$ and $\xi_1=\eta_1=0.5b$), cut off region position is occurred at h_1/h=0.3. Results on the pure global buckling load normalized with respect to P^*_{cr}=3.0396 versus c_1/b (c_1=0.1b with x_1=0.4b, x_2=0.5b, x_3=0.6b; c_1=0.2b with x_1=0.3b, x_2=0.5b, x_3=0.7b; c_1=0.3b with x_1=0.1b, x_2=0.5b, x_3=0.9b) are shown in Figure 5. The result show that normalized pure global buckling load ratio P_{cr}/P^*_{cr} decreases as the cut off region size P_{cr}/P^*_{cr} increases.

A square plate has arbitrary shape of typical cut off region with the coordinates $X_1(0.2b,0.2b)$, $X_2(0.8b,0.2b)$, $X_3(0.8b,0.8b)$, $X_4(0.5b,0.6b)$, $X_5(0.2b,0.4b)$ i.e., $c_1=d_1=0.3b$, $\xi_1=\eta_1=0.5b$. Results on the pure global buckling load normalized with respect to $P^*_{cr}=3.0396$ versus h_1/h are shown in Figure 6. The results show that normalized pure global buckling load ratio P_{cr}/P^*_{cr} firstly decreases then keeps almost constant as the cut off region position h_1/h increases.

In the case of vibration, we define the

non-dimensional frequency $k = b^2\omega\sqrt{\rho/D_{11}}$. . A plate without cut off region, the fundamental frequency for is found to be 2.42204. A square plate has arbitrary shape of typical cut off region with the coordinates $X_1(0.2b,0.2b)$, $X_2(0.6b,0.2b)$, $X_3(0.6b,0.8b)$, $X_4(0.4b,0.6b)$, $X_5(0.2b,0.4b)$ i.e. $c_1 = 0.2b, d_1 = 0.3b$, $\xi_1 = 0.4b, \eta_1 = 0.5b$, cut off region position is occurred at h_1/h= 0.3. Results on the non-dimensional fundamental frequency k versus P/P_{cr}^0 are shown in Figure 7. The result shows that the decreases as the P/P_{cr}^0 increases.

3.1.2 Clamped plate

For a clamped rectangular plate without cut off region, the critical buckling load is $P_{cr}^0 = 6.9477$, this value should be the maximum upper bound for all other numerical results presented for a clamped plate. A square plate has arbitrary shape of typical cut off region with y-coordinates y_1=0.2b, y_2=0.4b, y_1=0.6b, y_2=0.8b, (fixed d_1=0.3b and ζ_1=η_1=0.5b,), cut off region position is occurred at h_1/h= 0.3. Results on the critical load normalized with respect to $P_{cr}^0 = 6.9477$ versus c_1/b (c_1=0.1b, with x_1=0.4b, x_2=0.5b, x_3=0.6b; c_1=0.2b with x_1=0.3b, x_2=0.5b, x_3=0.7b; c_1=0.3b with x_1=0.2b, x_2=0.5b, x_3=0.8b; c_1=0.4b with x_1=0.1b, x_2=0.5b, x_3=0.9b) are shown in Figure 8. The result show that normalized pure global buckling load ratio P_{cr}/P_{cr}^0 decreases as the cut off region size c_1/b increases.

A square plate has arbitrary shape of typical cut off region with the coordinates x_1(0.2b, 0.2b), x_2(0.6b, 0.2b), x_3(0.6b, 0.8b), x_4(0.4b, 0.6b), x_5(0.2b, 0.4b) i.e. c_1=0.2b, d_1=0.3b, ζ_1=0.4b, η_1=0.5b, Results on the pure global buckling load normalized with respect to $P_{cr}^0 = 6.9477$ versus h_1/h are shown in Figure 9. The result show that normalized pure global buckling load ratio P_{cr}/P_{cr}^0 firstly decreases and then keeps almost constant as the cut off region position h_1/h increases.

A plate without cut off region, the fundamental frequency for k is found to be 3.20406. A square plate having arbitrary shape of typical cut off region with the

coordinates $x_1(0.2b, 0.2b)$, $x_2(0.6b, 0.2b)$, $x_3(0.6b, 0.8b)$, $x_4(0.4b, 0.6b)$, $x_5(0.2b, 0.4b)$ i.e. $c_1=0.2b$, $d_1=0.3b$, $\zeta_1=0.4b$, $\eta_1=0.5b$, cut off region position is occurred at $h_1/h=0.3$. Results on the non-dimensional fundamental frequency k versus P/P^*_{cr} are shown in Figure 10. The results show that the k decreases as the P/P^*_{cr} increases.

3.2 Circular cut off region case

For a square plate has a circular cut off region centered at $\xi_1=\eta_1=0.5b$ and cut off region radius $r=0.3b$ that is shown in Figure 11. We partition the circular cut off region into rectangular shape of twelve sub-regions and right triangular shape of twelve sub-regions with coordinates $X_1(x_1, y_1)$ to $X_{12}(x_{12}, y_{12})$ corresponding to x- and y-coordinates $x=\xi_1+r\cos\theta$, $y=\eta_1+r\sin\theta$, where $\theta=n\pi/6$ and n is integer, that is shown in Figure 12. Some numerical results are presented for four sides simply-supported plate as well as clamped plate under the global buckling and vibration.

3.2.1 Simply supported plate

Results on the pure global buckling load normalized with respect to $P^*_{cr}=6.9477$ versus h_1/h were shown in Figure 13. The result show that normalized pure global buckling load ratio P_{cr}/P^*_{cr} decreases as the cut off region position h_1/h increases. Results on the non-dimensional fundamental frequency k versus were shown in Figure 14. The results show that the decreases as the P/P^*_{cr} increases.

3.2.2 Clamped plate

Result on the pure global buckling load normalized with respect to $P^*_{cr}=6.9477$ versus h_1/h was shown in Figure 15. The result show that normalized pure global buckling load ratio P_{cr}/P^*_{cr} decreases as the cut off region position h_1/h increases. Result on the non-dimensional fundamental frequency k versus P/P^*_{cr} was shown in Figure 16. The results show that the k decreases as the P/P^*_{cr} increases.

3.3 Elliptical cut off region case

For a square plate has an elliptic cut off region centered at $\xi_1=\eta_1=0.5b$ and cut off region length $c_1=0.3b$, aspect ratio $R=d_1/c_1$, as shown in Figure 17.

Similarly, we partition the elliptic cut off region into rectangular shape of twelve sub-regions and right triangular shape of twelve sub-regions with coordinates $X_1(x_1, y_1)$ to $X_{12}(x_{12}, y_{12})$ corresponding to x- and y- coordinates , $x = \xi_1 + c_1 \cos\theta$, $y = \eta_1 + d_1 \sin\theta$ where $\theta = n\pi/6$ and n is integer. Some numerical results are presented for four sides simply supported plate as well as clamped plate under the pure global buckling and vibration.

3.3.1 Simply supported plate

Results on the pure global buckling load normalized with respect to P^*_{cr}=3.0396 versus for h_1/h for R=0.5~1.0 was shown in Figure 18. The result show that normalized pure global buckling load ratio P_{cr}/P^*_{cr} decreases as the cut off region position h_1/h increases. The non-dimensional fundamental frequency k versus P/P^*_{cr} for $R = 0.5 \sim 1.0$ was shown in Figure 19. The result show that the k decreases as the P/P^*_{cr} increases.

3.3.2 Clamped plate

Results on the pure global buckling load normalized with respect to P^*_{cr}=6.9477 versus h_1/h for R=0.5~1.0 was shown in Figure 20. The result show that normalized pure global buckling load ratio P_{cr}/P^*_{cr} decreases as the cut off region position h_1/h increases. The non-dimensional fundamental frequency k versus P/P^*_{cr} for for R=0.5~1.0 was shown in Figure 21. The result show that the k decreases as the P/P^*_{cr} increases.

4. Conclusions

The pure global buckling and vibration predictions due to reduced flexural stiffness effect for four sides simply supported as well as clamped anisotropic laminates having arbitrary shape of cut off region have been studied by treating the cut off region with reduced stiffness. The stiffness variation of the plate is represented by Fourier series. The numerical results are obtained by the Ritz method of energy approach for plates having typical arbitrary shape of cut off region and utilizing the partition technique

under biaxial compression loads. We find that the normalized pure global buckling load ratio P_{cr}/P^{0}_{cr} decreases as the cut off region size increases. The non-dimensional fundamental frequency k decreases as the P/P^{0}_{cr} increases.

References

1. Timoshenko, S. P. and Gere, J. M., "Theory of Elastic Stability," McGrow-Hill Book Company, 1981
2. Wang, S. S., Zahlan N. M. and Suemasu H., "Compressive Stability of Delaminated Random Short-Fiber Composites, Part I: Modeling and Methods of Analysis," Journal of Composite Materials, Vol.19, pp. 296-316, 1985
3. Wang, S. S., Zahlan N. M. and Suemasu H., "Compressive Stability of Delaminated Random Short-Fiber Composites, Part II: Experimental and Analytical Results," Journal of Composite Materials, Vol.19, pp. 317-333, 1985
4. Simitses, G. J., Sallam, S. and Yin, W. L., "Effect of Delamination of Axially Loaded Homogeneous Laminated Plates," AIAA Journal, Vol.23, No.9, pp.1437-1444, 1985
5. Wang, J. T.-S., Lin, C. C. and Ong, C. L., "Analysis of Delaminated Composite Structures II," Project Report No. NSC 83-0401-0-005-001, Dept. of Applied Math., National Chung Hsing University, Taiwan, 1994
6. Jane, K. C., and Hong, C. C., "Buckling and Vibration of Rectangular Laminates with Cut Off Regions," Mechanics Research Communications, Vol. 27, No. 1, pp. 101-108, 2000
7. Whitney, J. M., "Structural Analysis of Laminated Anisotropic Plates," Technomic Publishing Company, Inc., 1987
8. Szilard, R., "Theory and Analysis of Plates Classical and Numerical Methods," Prentice-Hall, Inc., Englewood Cliffs. New Jersey, 1974

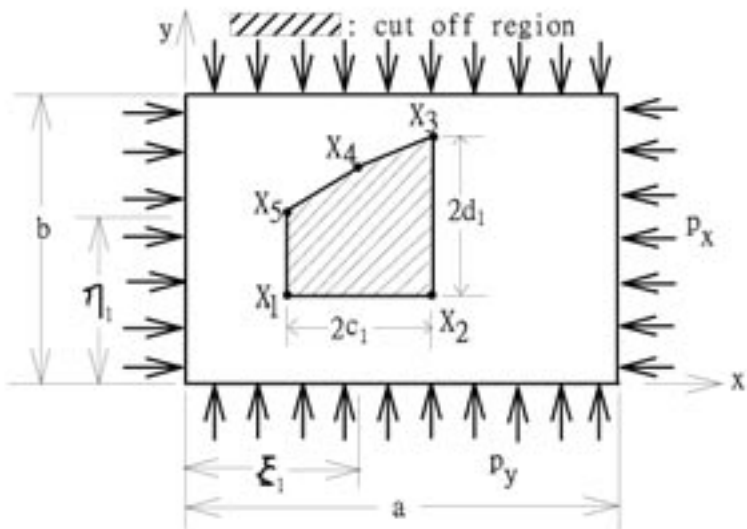

Figure 1 Geometry of a typical laminated plate with arbitrary shape of cut off region

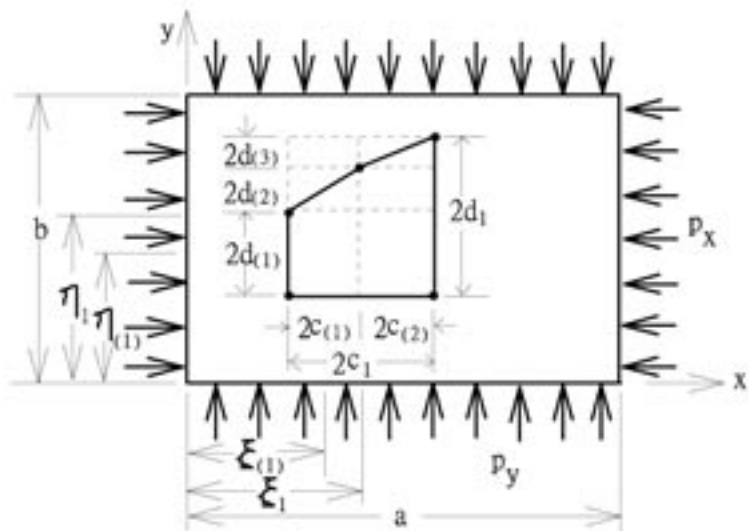

Figure 2 The sub-regions of approximately arbitrary shape cut off region

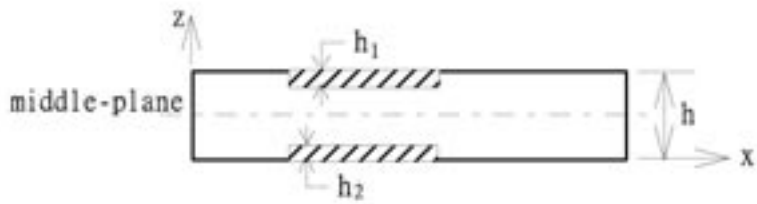

Figure 3 Typical thickness position of cut off region

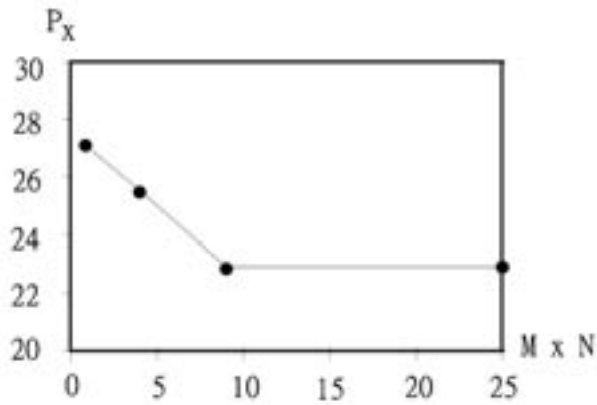

Figure 4a Simply supported plate with arbitrary shape of typical cut off region

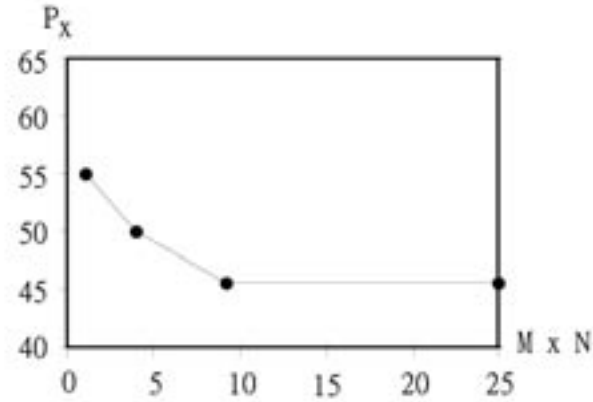

Figure 4b For a clamped plate with arbitrary shape of typical cut off region

Figure 4 Convergence of pure global buckling solution

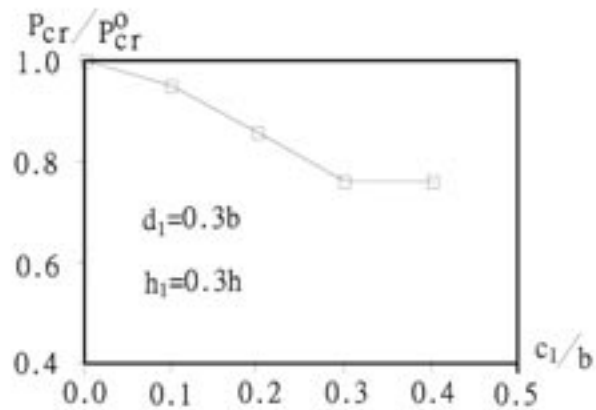

Figure 5 The pure global buckling load vs. cut off region size

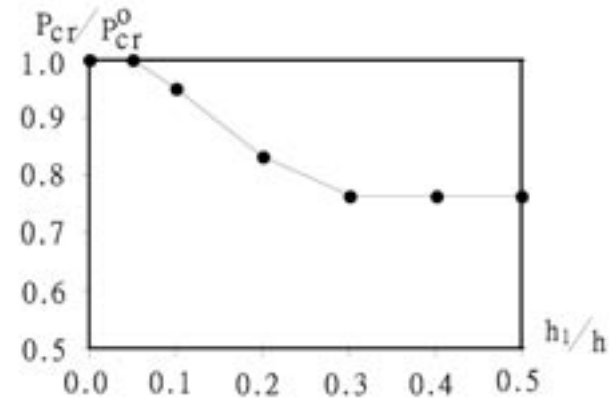

Figure 6 The pure global buckling load vs. cut off region position

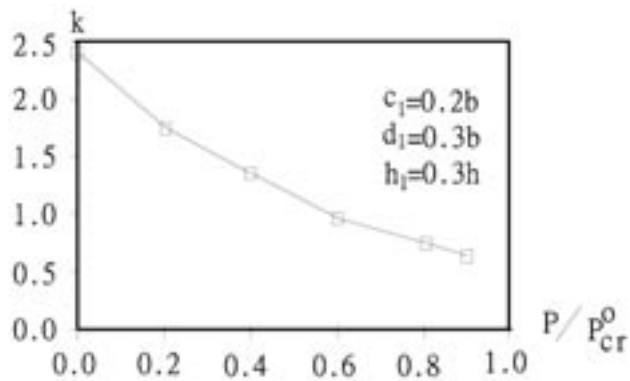

Figure 7 The fundamental frequency vs. axial load

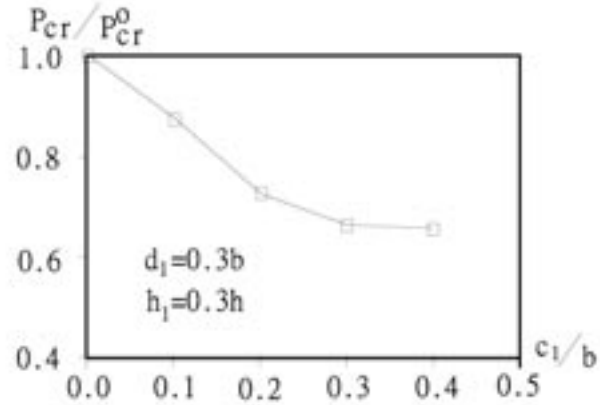

Figure 8 The pure global buckling load vs. cut off region size for a clamped plate

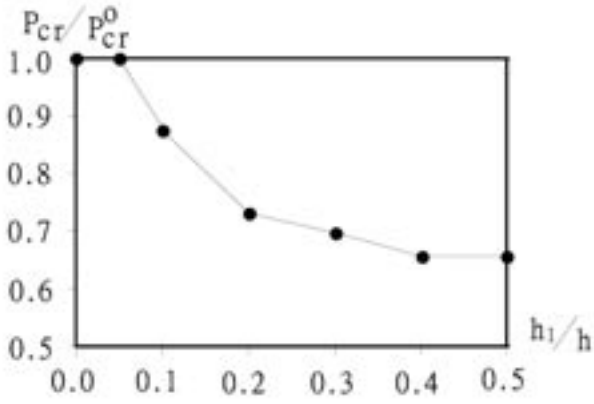

Figure 9 Pure global buckling load vs. cut off region position for a clamped plate

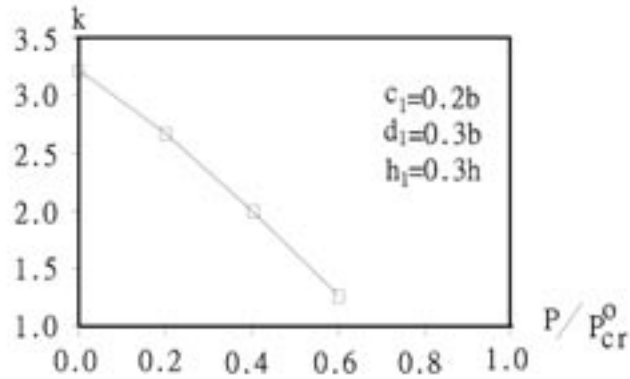

Figure 10 The fundamental frequency vs. axial load for a clamped plate

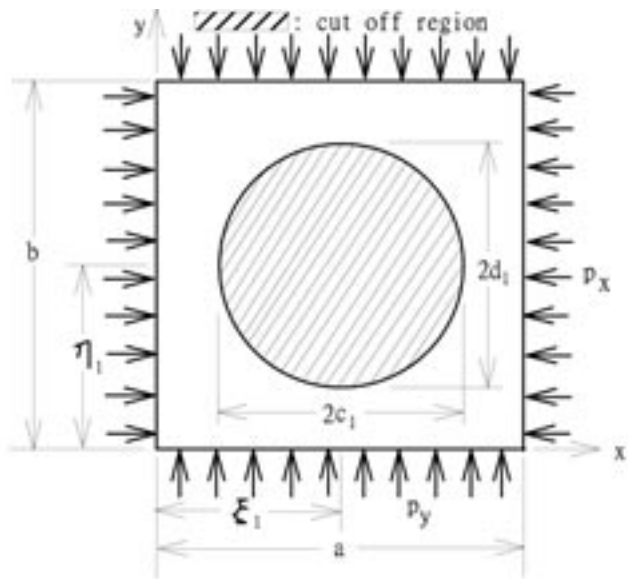

Figure 11 Geometry of a plate with circular cut off region

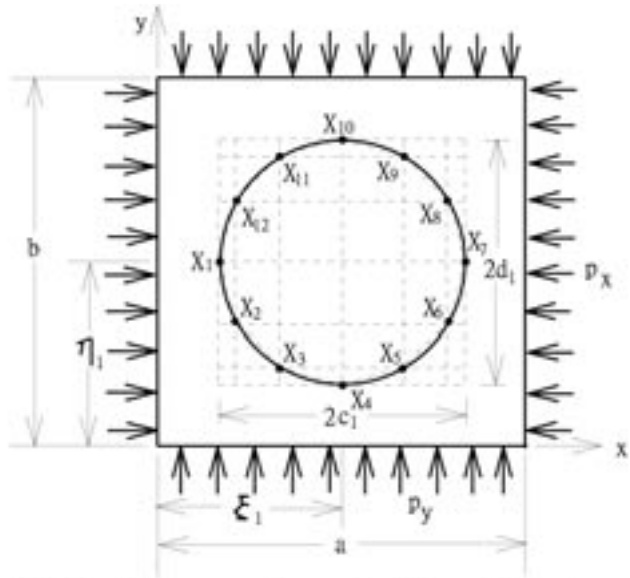

Figure 12 The sub-regions of approximately cut off region

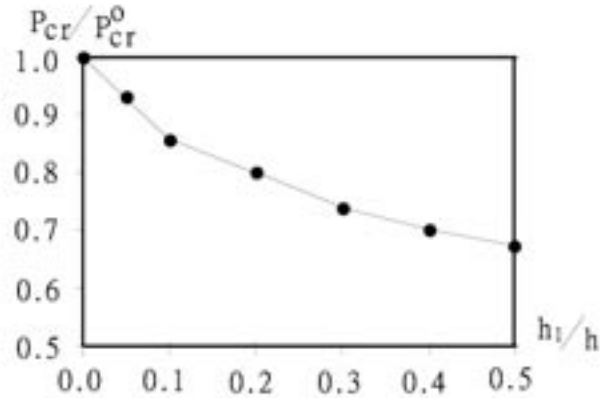

Figure 13 Pure global buckling load vs. circular cut off region position in simply-supported plate

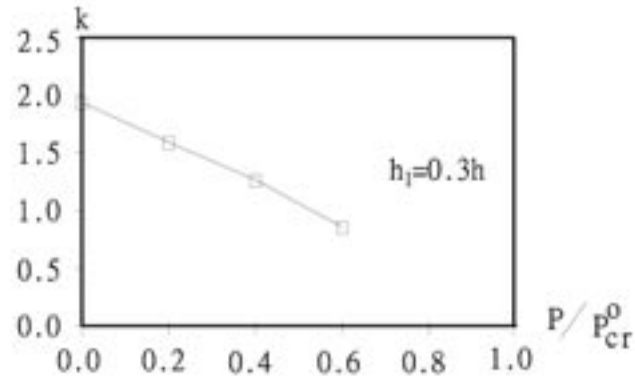

Figure 14 Fundamental frequency vs. axial load for a circular cut off region in simply supported plate

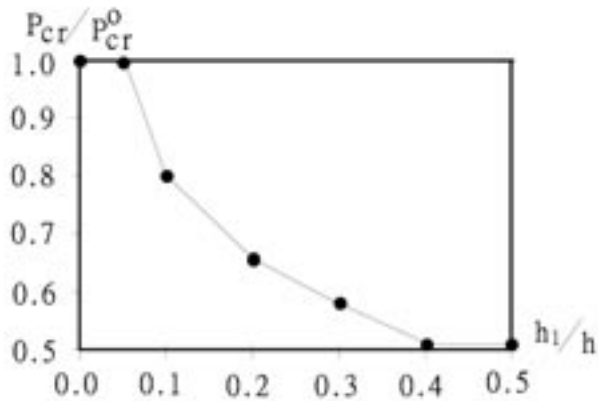

Figure 15 The pure global buckling load vs. circular cut off region position for a clamped plate

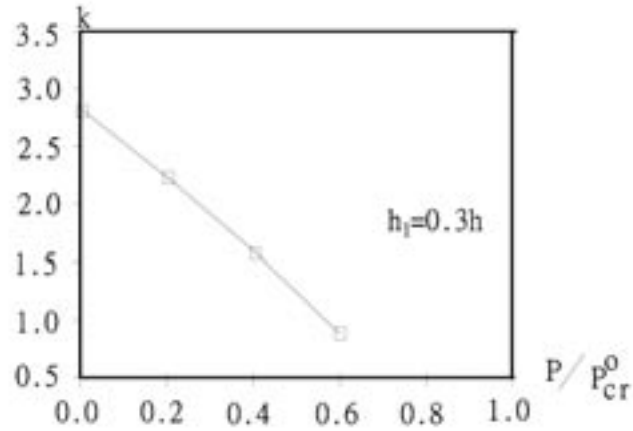

Figure 16 The fundamental frequency vs. axial load for a circular cut off region in clamped plate

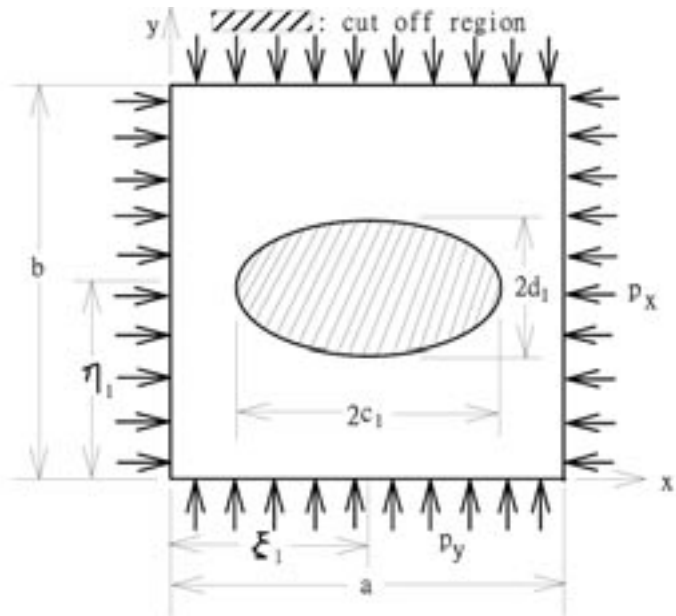

Figure 17 Geometry of a plate with elliptical cut off region

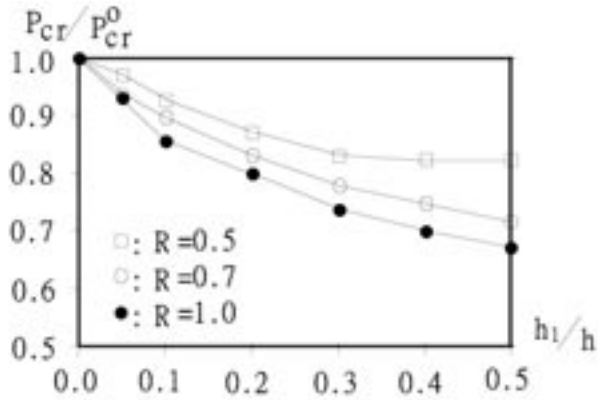

Figure 18 Pure global buckling load vs. elliptical cut off region position in simply supported plate

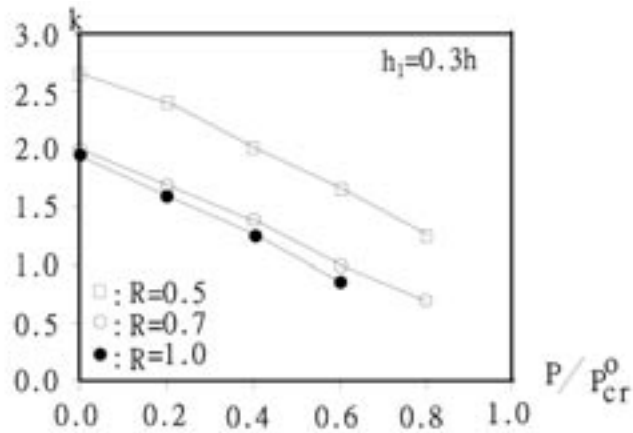

Figure 19 The fundamental frequency vs. axial load for elliptical cut off region in a simply supported plate

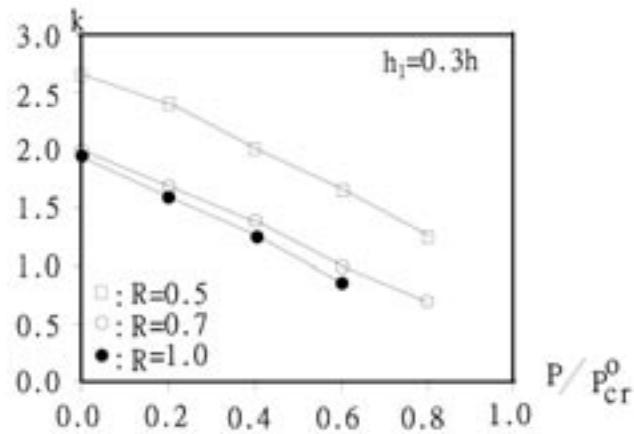

Figure 19 The fundamental frequency vs. axial load for elliptical cut off region in a simply supported plate

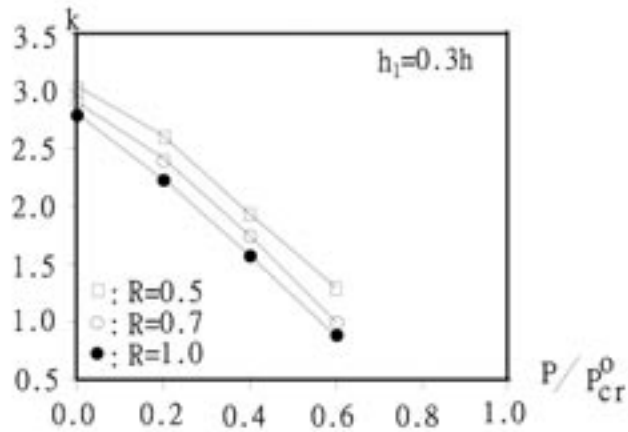

Figure 21 The fundamental frequency vs. axial load for elliptical cut off region for a clamped plate